Leaky Lamb waves in an anisotropic plate. I: An exact solution and experiments

Vinay Dayal, and Vikram K. Kinra

Citation: The Journal of the Acoustical Society of America **85**, 2268 (1989);
View online: https://doi.org/10.1121/1.397772
View Table of Contents: http://asa.scitation.org/toc/jas/85/6
Published by the Acoustical Society of America

Leaky Lamb waves in an anisotropic plate. I: An exact solution and experiments

Vinay Dayal
Aerospace Engineering Department, Iowa State University, Ames, Iowa 50011

Vikram K. Kinra
Department of Aerospace Engineering and Mechanics and Material Center, Texas A&M University, College Station, Texas 77843

(Received 22 June 1988; accepted for publication 23 February 1989)

The propagation of leaky Lamb waves in a plate consisting of a general balanced symmetric composite material is considered. The problem has been examined both analytically as well as experimentally. An exact solution for the dispersion equation was obtained. Numerical results for complex-valued wavenumber were obtained for an isotropic material (aluminum) and a $(0/90_3)_s$ graphite/epoxy laminate. Excellent agreement for the isotropic case and a satisfactory agreement for the anisotropic case between the theory and experiment were observed.

PACS numbers: 43.20.Fn, 43.35.Pt

INTRODUCTION

Lamb waves are waves propagating in the plane of a plate with traction-free boundaries. In the case of plane Lamb waves, the particle displacement is in two directions: (1) the wave propagation direction and (2) the thickness direction. The third component is zero because the plate is considered infinite in the plane of the plate. The governing equations for the Lamb waves were first derived by Professor Horace Lamb in 1917 in his famous work.[1] These equations were quite complicated and a solution could be obtained only in the short and long wavelength limits. In 1945, Osborne and Hart[2] dealt with the problem of waves generated by an underwater explosion interacting with steel plates. First, a comprehensive solution of Lamb waves was obtained by Mindlin[3] in 1950. Later, Viktorov[4] in his book dealt with the solution of Lamb waves in great detail. He provided the dispersion curves for a material with a Poisson's ratio of 0.34. According to Viktorov[4] and Krautkramer *et al.*,[5] the dispersion equations for Lamb waves in a plate immersed in a fluid were derived by Schoch.[6] Merkulov[7] has shown that if the density of the plate is large compared to that of the immersion fluid, then the inertia effect of the fluid is negligible. He obtained a first-order approximation solution for the complex part of the wavenumber, i.e., attenuation. Plona *et al.*[8] have shown that, when the plate density is comparable to the fluid density, as in the case of Plexiglas in water for example, then the inertial effects are significant and cannot be neglected.

Most of the work on Lamb waves has been motivated by the ultrasonic flaw detection of sheet material. Worlton[9] experimentally observed the existence of Lamb waves at Megacycle frequencies, and Dragonette[10] produced some excellent visual pictures of the Lamb wave phenomenon by Schlieren technique. Various other researchers have studied the Lamb waves and used them for nondestructive evaluation (NDE) of homogeneous plates.[11–15] This is by no means an exhaustive list of the work in this field. With the advent of composites as a major structural material, especially in the aerospace industry, the attention of the NDE community has shifted toward the composites, and many of the NDE tools available for the testing of isotropic materials have been applied to the composites. Quite naturally, ultrasonics has also been used for the NDE of composites with varying degrees of success. The major difficulty in case of the composites arises from the fact that the theoretical analysis of wave propagation is considerably more difficult. For example, in an isotropic material, the wave propagation and energy propagation directions are the same; in an anisotropic material, the two are, in general, quite different.

The general elastic wave problem in a layered composite is very complex, and an exact solution is neither possible nor needed. Various simplified theories have been proposed, which tend to make the calculation of dispersion relations manageable. The simplest ones to be proposed were the effective modulus theories.[16–18] Here, the geometrically weighted average of the constituent properties are used as the average material constants. Habegar *et al.*[18] have replaced the composite plate with an equivalent homogeneous anisotropic plate and derived the Lamb wave displacement relations using the effective stiffness matrix. They have utilized these equations for the measurement of the nine elastic constants of paper.[19]

Some models[20–22] have been proposed to account for the dynamic effects of the propagating wave in the plates. These models incorporate the influence of the microstructure and anisotropy. One such "effective stiffness" theory was proposed by Sun *et al.*[20] The fiber and matrix displacements are expressed as linear expansion about the midplanes of the layers. The continuity relations take into account the dynamic interaction of the layers. Bedford *et al.*[21] have proposed a diffusing continuum theory where the constituents are modeled as superimposed continua that undergo individual deformations. These deformations are then coupled together in a dynamical process. The theory proposed by Chementi and Nayfeh[22] calculates the effective homogeneous

 0001-4966/89/062268-09$00.80

transverse isotropic elastic behavior of a unidirectional composite in the long wavelength limit, using a two-step procedure based on alternating layered media. These results were then applied to a fluid-loaded anisotropic plate, which is assumed to approximate the unidirectional fibrous composite laminate. The first limitations in all these theories is that they only consider ideal unidirectional composites with waves traveling in the fiber direction. Practical laminates, however, are cross-ply and angle-ply laminates, and the effect of waves in these laminates becomes extremely complicated. The second limitation is that these theories have not considered the effect of fluid immersion and, hence, attenuation due to the leakage into the surrounding medium has been neglected.

As noted earlier, Habegar[18] calculated the dispersive equations for a balanced symmetrical laminate in vaccuum (i.e., traction-free boundary conditions). The object of the present work is to extend his analysis to the case of a laminate immersed in a liquid. The equations have been written in a form so that they can be used in conjunction with the effective stiffness matrix generated by any theory. The composite plate is replaced by an equivalent homogeneous anisotropic plate. Closed-form dispersion equations are derived for both the symmetric and antisymmetric modes of Lamb wave propagation; an exact numerical solution is given. Due to particle displacement normal to the plate, waves are also set up in the surrounding fluid. This is the mechanism by which energy "leaks" from the plate into the liquid; hence, the term "leaky Lamb waves." At the risk of stating the obvious, the wavenumber is complex; the imaginary part is the attenuation and is a measure of the energy leaked into the liquid. Stiffness matrix calculated from the "effective modulus" theory has been used for the results presented here. Theoretical results obtained from the dispersion equation have been experimentally verified by tests performed on steel and aluminum plates. Excellent comparison between the theory and experiments was obtained. Finally, the theoretical solution for a composite laminate has been verified by tests performed on a $(0/90_3)_s$ graphite/epoxy composite plate.

I. THEORY

The development of the dispersion equations has traditionally been approached in two different ways. First, as developed by Lamb, the particle displacement U is written in terms of a scalar and a vector potential. A plane harmonic wave propagating in the plane of the plate is assumed, which allows the potential to be written so that the separation of variables technique can be used. The solution of potential equations is then used to satisfy the boundary conditions and the dispersion equation, linking wave speed and frequency, is obtained. The second approach, namely, the method of partial waves, is more recent and is followed by Achenbach.[23] Harmonic waves can travel in a plate by reflecting back and forth between the two plane surfaces. These waves combine in such a manner that in the steady state a wave which consists of a traveling wave in the plane of plate and a standing wave in the thickness direction is obtained. This approach is more fundamental in that it directly provides the wave solution and results in a clearer picture of the nature of the wave propagation. In the following, the second approach has been used. Since all the tests are performed under water, wave propagation in a plate immersed in a fluid is considered and suitable boundary conditions are applied.

A liquid-borne longitudinal wave incident on an unbounded plate is shown in Fig. 1. Shown also are the mode-converted longitudinal and shear waves in the plate. The waves in the liquid along with the waves in the plate must sustain themselves to form a steady-state wave pattern in the plate. The conditions of the continuity of the displacements and equilibrium of forces at the plate–fluid interface have to be satisfied. The coordinate directions used here are the standard ones used in the composites literature: directions 1 and 2 in the plane of the plate while 3 normal to it.

For any symmetrical composite laminate, the stress–strain relation can be written as

$$\begin{pmatrix}\sigma_{11}\\ \sigma_{22}\\ \sigma_{33}\\ \sigma_{23}\\ \sigma_{31}\\ \sigma_{12}\end{pmatrix} = \begin{pmatrix} C_{11} & C_{12} & C_{13} & 0 & 0 & C_{16}\\ C_{21} & C_{22} & C_{23} & 0 & 0 & C_{26}\\ C_{31} & C_{32} & C_{33} & 0 & 0 & C_{36}\\ 0 & 0 & 0 & 2C_{44} & C_{45} & 0\\ 0 & 0 & 0 & C_{54} & 2C_{55} & 0\\ C_{61} & C_{62} & C_{63} & 0 & 0 & 2C_{66}\end{pmatrix} \begin{pmatrix}\epsilon_{11}\\ \epsilon_{22}\\ \epsilon_{33}\\ \epsilon_{23}\\ \epsilon_{31}\\ \epsilon_{12}\end{pmatrix}. \tag{1}$$

The strain displacement relation can be written as

$$\epsilon_{ij} = (U_{i,j} + U_{j,i})/2, \quad \text{for } i,j = 1,2,3. \tag{2}$$

The equation of motion in an elastic medium is

$$\sum_{j=1}^{3} \sigma_{ij,j} = \rho \ddot{U}_i, \quad i = 1,2,3. \tag{3}$$

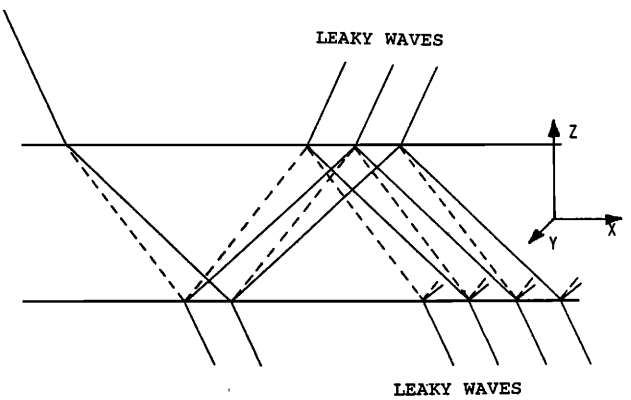

FIG. 1. Generation of Lamb waves in a plate. Each reflection produces a longitudinal (solid line) and a transverse (dash line) wave.

A plane wave traveling in an arbitrary direction **x** may be written as

$$\ddot{U} = U_0 \exp[i(\mathbf{k}\cdot\mathbf{x} - \omega t)], \tag{4}$$

where **U** is the displacement vector, U_0 its amplitude, and **k** is the wavenumber vector.

We now assume a plane strain condition considering an infinite plate. The displacement U_2 and all derivatives with respect to y vanish. Substituting Eqs. (1) and (2) in Eq. (3) yields

$$\rho\ddot{U}_1 = C_{11}U_{1,11} + C_{13}U_{3,31} + C_{55}(U_{1,33} + U_{3,13}), \tag{5}$$

$$\rho\ddot{U}_3 = C_{33}U_{3,33} + C_{13}U_{1,13} + C_{55}(U_{1,13} + U_{3,11}). \tag{6}$$

For a plane wave with displacements in the x and z directions only, the displacement components U_1 and U_3 can be written from Eq. (4), as

$$U_1 = U_{10} \exp[i(k_x x + k_z z - \omega t)] \tag{7}$$

and

$$U_3 = U_{30} \exp[i(k_x x + k_z z - \omega t)]. \tag{8}$$

where U_{10} and U_{30} are the wave amplitudes. Substituting Eqs. (5) and (6) in Eqs. (7) and (8) one obtains

$$\rho U_{10}\omega^2 = C_{11}U_{10}k_x^2 + (C_{55} + C_{13})U_{30}k_x k_z + C_{55}U_{10}k_z^2 \tag{9}$$

and

$$\rho U_{30}\omega^2 = C_{55}U_{30}k_x^2 + (C_{55} + C_{13})U_{10}k_x k_z + C_{33}U_{30}k_z^2. \tag{10}$$

Let us define R as

$$R = U_{30}/U_{10}$$

$$= (\rho\omega^2 - C_{11}k_x^2 - C_{55}k_z^2)/(C_{55} + C_{13})k_x k_z. \tag{11}$$

Eliminating U_{10} and U_{30} from Eqs. (9) and (10), we get a quadratic equation for k_z in terms of k_x and the elastic constants as

$$k_z^2 = k_x^2[-B \pm (B^2 - 4D)^{1/2}]/2, \tag{12}$$

where

$$B = \left[\frac{C_{33}}{\rho}\left(\frac{C_{11}}{\rho} - \frac{\omega^2}{k_x^2}\right) - \frac{C_{13}}{\rho}\frac{2C_{55} + C_{13}}{\rho} - \frac{C_{55}\omega^2}{\rho k_x^2}\right] \Big/ \frac{C_{33}C_{55}}{\rho^2}$$

and

$$D = \frac{\omega^2}{k_x^2} - \frac{C_{55}}{\rho}\frac{\omega^2}{k_x^2} - \frac{C_{11}}{\rho} \Big/ \frac{C_{33}C_{55}}{\rho^2}.$$

Let us define k_{zp} and k_{zm} as the two values of k_z obtained from Eq. (12) with + or − signs. Also, R_p and R_m will be the value of R when k_{zp} and k_{zm}, respectively, are substituted in Eq. (11). The equations derived above are for bulk waves traveling in an unbounded medium. These bulk waves traveling in the plate add up, such that, subject to the proper boundary conditions, the plate wave solution is obtained. The two possible plate wave displacements have the following forms:

$$U_1 = \exp[i(k_x x - \omega t)][M\exp(ik_{zp}z) + N\exp(-ik_{zp}z) + P\exp(ik_{zm}z) + Q\exp(-ik_{zm}z)], \tag{13}$$

$$U_3 = \exp[i(k_x x - \omega t)]\{R_p[M\exp(ik_{zp}z) - N\exp(-ik_{zp}z)] + R_m[P\exp(ik_{zm}z) - Q\exp(-ik_{zm}z)]\}, \tag{14}$$

where M,N,P,Q are arbitrary constants.

The boundary conditions to be satisfied for a plate of thickness $2d$ are

$$\sigma_{33} = C_{33}U_{3,3} + C_{13}U_{1,1} = -p, \quad \text{at } z = \pm d \tag{15}$$

and

$$\sigma_{31} = C_{55}U_{1,3} + C_{55}U_{3,1} = 0, \quad \text{at } z = \pm d. \tag{16}$$

That is, the normal stresses in the plate and the liquid are equal and the shear stresses on the plate surface are zero as the fluid does not sustain shear. In addition, the continuity of displacement demands,

$$U_3 = W_L, \quad \text{at } z = \pm d, \tag{17}$$

where W_L is the displacement in the liquid.

Substituting Eqs. (13) and (14) in Eqs. (15) and (16), the following set of equations is obtained:

$$MG_pX + NG_p/X + PG_m Y + QG_m/Y = ip(z = d), \tag{18a}$$

$$MG_p/X + NG_pX + PG_m/Y + QG_m Y = ip(z = -d), \tag{18b}$$

$$MH_pX - NH_p/X + PH_m Y - QH_m/Y = 0, \tag{18c}$$

$$MH_p/X - NH_pX + PH_m/Y - QH_m Y = 0, \tag{18d}$$

where

$$G_{p,m} = C_{33}k_{zp,m} + C_{13}k_x, \quad H_{p,m} = k_{zp,m} + k_x R_{p,m}$$

and

$$X = \exp(ik_{zp}d), \quad Y = \exp(ik_{zm}d).$$

The wave motion in the fluid satisfies the equation

$$\frac{\partial^2\phi_L}{\partial x^2} + \frac{\partial^2\phi_L}{\partial z^2} + k_L^2\phi_L = 0, \tag{19}$$

where $k_L = \omega/c_L$ is the wavenumber and c_L is the wave speed in the fluid. The form of the potential ϕ_L in the fluid to satisfy Eq. (19) is

$$\phi_L = \phi_0 \exp[i(k_x x + k_z z - \omega t)]. \tag{20}$$

Substituting Eq. (19) in Eq. (18), it can be readily shown that

$$k_z^2 = k_L^2 - k_x^2.$$

The potential ϕ_L corresponds to a wave in the fluid that propagates along the plate in the x direction and decays exponentially along the z direction. This wave in the fluid has to be compatible with the Lamb wave in the plate. It means that this wave must pursue a path along the x axis with a velocity equal to the phase velocity of the Lamb waves. The

displacement in the fluid W_L can be calculated from the potential by

$$W_L = \frac{\partial \phi_L}{\partial z} = ik_z\phi_0 \exp[i(k_x x + k_z z - \omega t)]. \quad (21)$$

Applying the boundary conditions Eq. (17) to Eqs. (14), (21), and (18b) we get

$$mM + nN + rP + sQ = ik_z\phi_0 \exp(ik_z d) \quad (22)$$

and

$$-nM - mN - sP - rQ = -ik_z\phi_0 \exp(-ik_z d), \quad (23)$$

where

$$m,n = \pm R_p \exp(\pm ik_{zp} d)$$

and

$$r,s = \pm R_m \exp(\pm ik_{zm} d).$$

From Eqs. (18c) and (18d), we can write

$$aM - bN + cP - eQ = 0, \quad (24)$$

$$bM - aN + eP - cQ = 0, \quad (25)$$

where

$$a,b = H_p \exp(\pm ik_{zp} d)$$

and

$$c,e = H_m \exp(\pm ik_{zm} d).$$

From Eqs. (24) and (25), we get

$$N = [(ae - bc)P + (be - ac)Q]/(a^2 + b^2) = N_1 P + N_2 Q \quad (26)$$

and

$$M = [(be - ac)P + (ae - bc)Q]/(a^2 + b^2) = N_2 P + N_1 Q \quad (27)$$

where $N_1 = (ae - bc)/(a^2 + b^2)$ and $N_2 = (be - ac)/(a^2 - b^2)$.

Substituting the values of M and N into Eqs. (22) and (23), we can write

$$(g + l)(P + Q) = ik_z\phi_0[\exp(ik_z d) + \exp(-ik_z d)], \quad (28)$$

where $g = mN_2 + nN_1 + r$ and $l = mN_1 + nN_2 + s$.

Similarly, substituting the values of M and N into Eqs. (18a) and (18b),

$$P + Q = i[p(z = d) + p(z = -d)]/(F_1 + F_2), \quad (29)$$

where

$$F_1 = N_2 G_p X + N_1 G_p / X + G_m Y;$$

$$F_2 = N_1 G_p X + N_2 G_p / X + G_m / Y.$$

Comparing Eq. (28) with Eq. (29) yields

$$\frac{p(z = d) + p(z = -d)}{F_1 + F_2} = \frac{k_z\phi_0[\exp(ik_z d) + \exp(-ik_z d)]}{(g + l)}. \quad (30)$$

The pressure in the fluid can be calculated from the potential ϕ_L from the relation

$$p = \lambda \left\{ \frac{\partial_L^2 \phi}{\partial x^2} + \frac{\partial_L^2 \phi}{\partial z^2} \right\}, \quad (31)$$

which gives

$$p(z = d) + p(z = -d) = -\lambda_L (k_x^2 + k_z^2)\phi_0[\exp(ik_z d) - \exp(-ik_z d)]. \quad (32)$$

Substituting Eq. (32) in Eq. (30) yields

$$[k_L^2 - k_x^2]^{1/2}/(g + l) + \rho_L \omega^2/(F_1 + F_2) = 0.$$

Simplifying $F_1 + F_2$ and $g + h$, substituting into Eq. (33), and rearranging the equations give, for the symmetric mode,

$$\frac{\tan(k_{zp} d)}{\tan(k_{zm} d)} - \frac{G_p H_m}{G_m H_p} + \frac{i\rho_L \omega^2 \tan(k_{zm} d)}{\rho(G_m/\rho)[k_x^2 - k_L^2]^{1/2}} \times [-(H_m/H_p)R_p + R_m] = 0. \quad (34)$$

Similarly, we can show that, for the antisymmetric mode, the governing equation is

$$\frac{\tan(k_{zm} d)}{\tan(k_{zp} d)} - \frac{G_p H_m}{G_m H_p} + \frac{i\rho_L \omega^2 \cot(k_{zp} d)}{\rho(G_m/\rho)[k_z^2 - k_L^2]^{1/2}} \times [(H_m/H_p)R_p - R_m] = 0. \quad (35)$$

It is quite laborious, but not difficult, to show that, for an isotropic material, Eqs. (34) and (35) reduce to the equations (II.43) and (II.44) obtained by Viktorov.[4]

The first two terms of Eqs. (34) and (35) represent the dispersion relations for composite plate in vacuum. The third or the complex part of the equations is due to the immersion of plate in a liquid. It is observed that almost all factors in the equations are complex and the required root k_x is also complex. These complex transcendental equations were solved by a numerical algorithm, which is described next.

II. SOLUTION METHODOLOGY FOR DISPERSION EQUATIONS

The solutions of the dispersion equations for composite plates immersed in a fluid are obtained by the following two-step procedure.

(i) The correct value of k, of course, is complex. However, as a point of departure, k is taken to be real and the dispersion equation for a plate in air is used. In other words, the imaginary part of Eqs. (34) and (35) is ignored. The roots for the remaining equation are obtained by a linear search method. The search is conducted in small steps varying either the wave speed or the frequency while keeping the other fixed. Both modes of search are useful depending on the gradients of the dispersion curves in a particular region. The roots are then calculated precisely by the bisection technique.[24]

(ii) In the second step, a search is made for the complex roots of k, i.e., for

$$k = k_1 + ik_2. \quad (36)$$

Substituting in the complete dispersion equation (34) or (35) for an immersed plate, we can write these equations in the form

$$\mathrm{Re}(k_1,k_2) + i\,\mathrm{Im}(k_1,k_2) = 0, \tag{37}$$

where Re and Im are the real and imaginary parts of the dispersion equation. Now, for a solution to exist, both the real and imaginary parts must be simultaneously zero; i.e.,

$$\mathrm{Re}(k_1,k_2) = 0 \tag{38}$$

and

$$\mathrm{Im}(k_1,k_2) = 0. \tag{39}$$

Thus we have two transcendental equations with two unknowns k_1 and k_2. The modified Newton's (Secant) method is used to arrive at the roots of these equations. The initial estimate of the roots is k_1 as obtained from step one (k_1 for the Lamb wave in the plate in air) and $k_2 = 0$. Now, k_1 is incremented in steps of 0.1 and k_2 in steps of 0.01. Since the Newton's method converges quadratically, the roots are obtained fairly rapidly. The nature of these equations is quite complicated and, at places, roots are close together. It is difficult to study the uniqueness and convergence of all the roots for such a complicated equation. Hence, it is quite possible that depending on the gradient of the equations and roots being close to each other, the solution may converge to some nearby root. To guard against this occurrence, we drew the complete dispersion curve diagram. It was found that, in general, the convergence was unique and rapid. Only at a few points the solution did not converge and sometimes it would converge at a nearby root. These points could be easily identified from the dispersion diagrams by using the following criterion: Since the dispersion curves in air are smooth, it is reasonable to expect that the dispersion curves for the plate immersed in the fluid will also be smooth.

In the foregoing, the effective elastic moduli of the plate were calculated using the classical laminate theory. Heuristically, when the wavelength is very large compared to the plate thickness, one would expect our calculations to be a fairly accurate representation of the reality. On the other extreme, when the wavelength is short compared to the plate thickness and, more importantly, where it is comparable to the plate thickness, clearly the theory is expected to break down, for now the wave begins to "see" the individual plies. A question of practical significance is: Where does the transition occur? A systematic examination of the issue is beyond the scope of the work. However, in the following, we have proved this issue to a limited extent. This was the motivation for carrying out the experiments described next. It will be shown that the elementary "rule of mixtures" theory gives surprisingly good results up to $k_t d = 3.5$, where k_t is the shear wavenumber.

III. EXPERIMENTAL PROCEDURE

Shown in Fig. 2 is a block diagram of the experimental setup. The pulse generator produces a trigger signal, which is used to trigger the signal generator and also set the initial time ($t = 0$) for the digitizing oscilloscope. The signal generator is used to produce a tone burst, which is about 10–20 cycles long. This wavetrain is amplified to about 200 V and fed into the transmitting transducer, which launches a longitudinal wave in water. This wave is mode converted into a leaky Lamb wave in the specimen. These leaky Lamb waves are sensed by the receiver, which can be placed on either side of the specimen; see Fig. 3. Only the transmission mode [Fig. 3(a)] was used in this work. The signal from the receiver is amplified to about 1 V and fed into a digital oscilloscope. All measurements are made with a reference peak near the center of the signal where it appears to have a steady state. Note that a single cycle of signal will not be able to establish a good Lamb wave. When 1 cycle of a sine wave is input into the transducer, due to the damping characteristics of the transducer, certain transient frequencies are produced. Since these frequencies do not correspond to the frequencies required to sustain Lamb waves in the plate, good

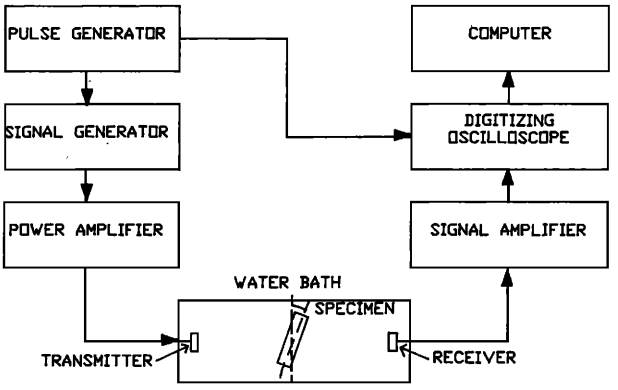

FIG. 2. Block diagram of the experimental setup.

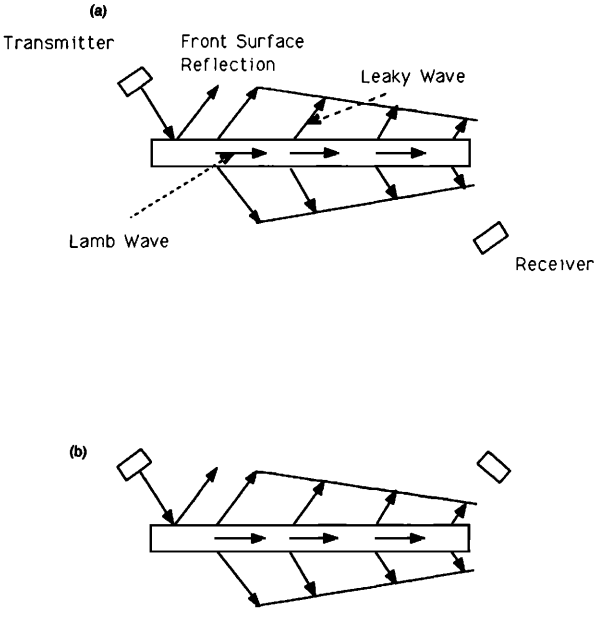

FIG. 3. Generation and reception of leaky Lamb waves: (a) Transmission and (b) reflection modes.

Lamb waves will not be produced. Hence, a long wavetrain is used that establishes the frequency of the signal and the effect of the transients can be ignored.

The transmitter and the receiver move on precision traveling mechanisms graduated to 0.001 in. The specimen is mounted on a turntable graduated to 0.1 deg. When the specimen is rotated, the transducers are moved accordingly so that the same length of the specimen is always interrogated. The specimen is rotated in small steps and the peak amplitude and location of a reference peak of the wave train is recorded.

The specimen is fixed at the angle identified as the Lamb angle for the measurement of attenuation. The receiver is moved by 0.5 (12.7 mm) in. in steps of 0.05 (1.27 mm) in. and the received signal is recorded. An exponential curve is fitted through this amplitude decay and the attenuation coefficient is estimated by the least-squares fit. The composite specimens tested during this work were fabricated using Magnamite AS4/3502 graphite/epoxy prepreg tapes manufactured by Hercules Inc.

IV. RESULTS AND DISCUSSION

The accuracy of our theory was checked in two ways: (1) against previous theories and (2) against our own experiments.

The dispersion equations for a steel plate in water were solved with $c_{11} = c_{22} = c_{33}$, $c_{12} = c_{13} = c_{23}$, and $c_{11} = (E/\rho)^2$, and a complex wavenumber was calculated. Figure 4(a) shows the dispersion curves for the steel plate. The solid lines are for the symmetric mode $(s_0, s_1, s_2, \ldots)$ and the dashed lines are for the asymmetric mode $(a_0, a_1, a_2, \ldots)$. Merkulov[7] did a corresponding analysis for an isotropic material but his solution was a first-order approximation. Even then, he was able to get good results because his assumption of $\rho_L/\rho \ll 1$ is valid for steel plate in water, where $\rho_L/\rho \cong 0.128$. Figure 4(b) shows the attenuation for the first two modes. The approximate solution obtained by Merkulov is also shown and is fairly close to our exact solution. In conclusion, the approximate analysis of Merkulov[7] serves to check our exact solution.

Next, the solution of the dispersive equations for an aluminum plate are presented in Fig. 5. (We note in passing that for aluminum $\rho_L/\rho = 0.37$, which is not negligible in comparison to one and, therefore, Viktorov's calculation may be quite inaccurate.) The dispersion curves are exactly as obtained by Viktorov[4] but attenuation curves cannot be compared since no earlier work is available. Next, we describe the experimental results obtained with an aluminum plate. For a fixed frequency $k_t d$, we measure the received amplitude as a function of the angle of incidence. The results are presented for three different values of $k_t d$ in Fig. 6. The peaks in the received signal correspond to the correct angle of incidence or "Lamb angle," which is governed by Snell's law:

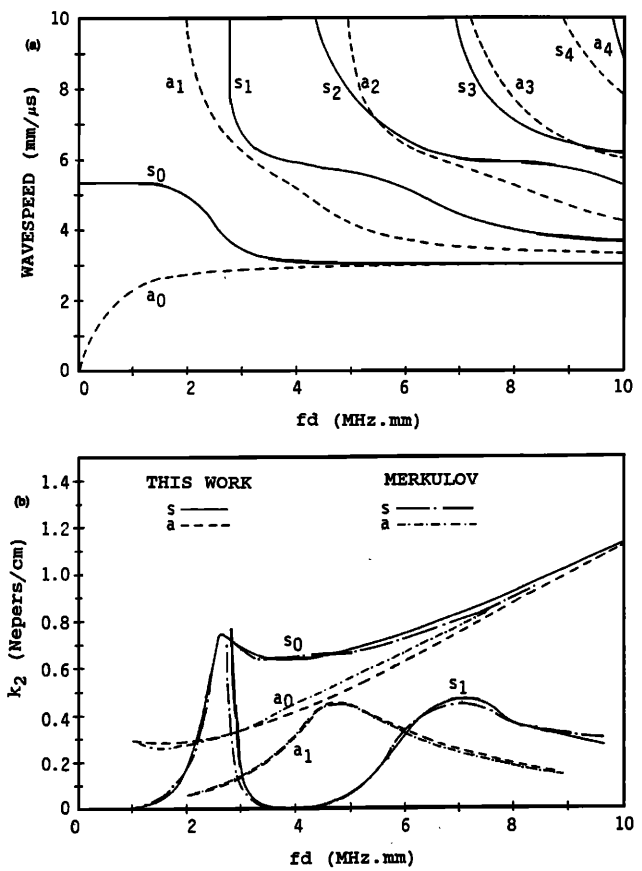

FIG. 4. (a) Dispersion curves and (b) attenuation curves for a steel plate immersed in water.

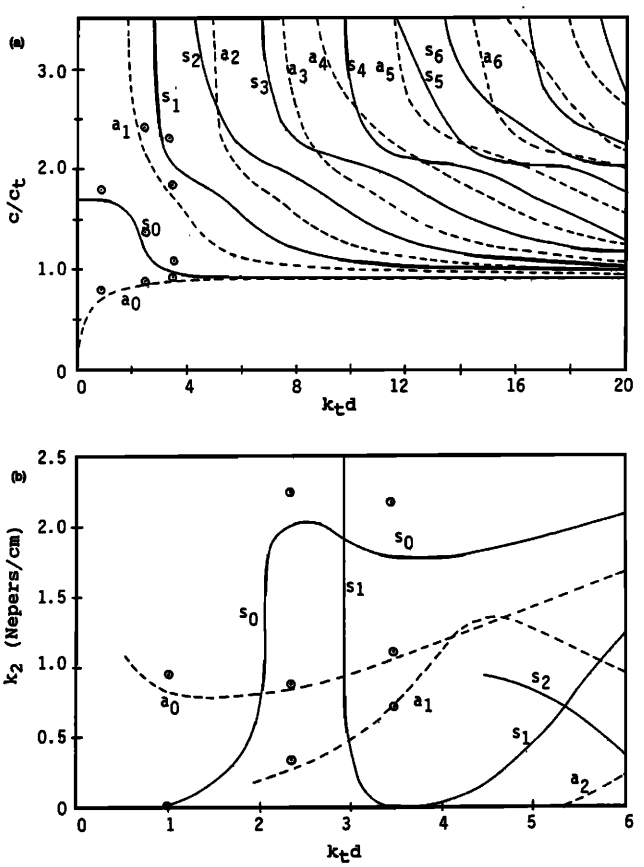

FIG. 5. (a) Dispersion curves and (b) attenuation curves for an aluminum plate immersed in water. Discrete points are experimental.

$$\sin(\theta_i)/\sin(\theta_r) = c_w/c_L, \tag{40}$$

where θ_i is the angle of incidence, θ_r is the angle of refraction ($=\pi/2$ for Lamb waves), c_w is the wave speed in water, and c_L is the Lamb wave speed. Thus

$$c_L = c_w/\sin(\theta_i). \tag{41}$$

It is noted, in Fig. 6(a), at $k_t d = 1.0$, that two peaks are obtained. Converted to wave speeds with Eq. (41), the values are shown as circled dots on the dispersion curves in Fig. 5(a). The same comment applies to peaks in Fig. 6(b) and (c). The attenuation was measured as described earlier. Measured values of the attenuation coefficient for an aluminum plate are shown as circles in Fig. 5(b). For the a_0 and a_1 modes, the agreement between theory and experiments is excellent. For the s_0 mode, the agreement is excellent as far as the lowest $k_t d$ (1.0) but becomes poorer as $k_t d$ increases. The reason for this becomes very clear when Figs. 5(b) and 6 are examined together: The attenuation of the s_0 mode increases very rapidly with $k_t d \cong 2.0$ [Fig. 5(b)]. This results in a correspondingly small received signal for the s_0 mode (Fig. 6) and a poor signal-to-noise ratio. Hence, a larger scatter in data is to be expected. The importance of calculating attenuation curves becomes apparent: Whenever possible, the tests should be performed at low attenuation values to get accurate results.

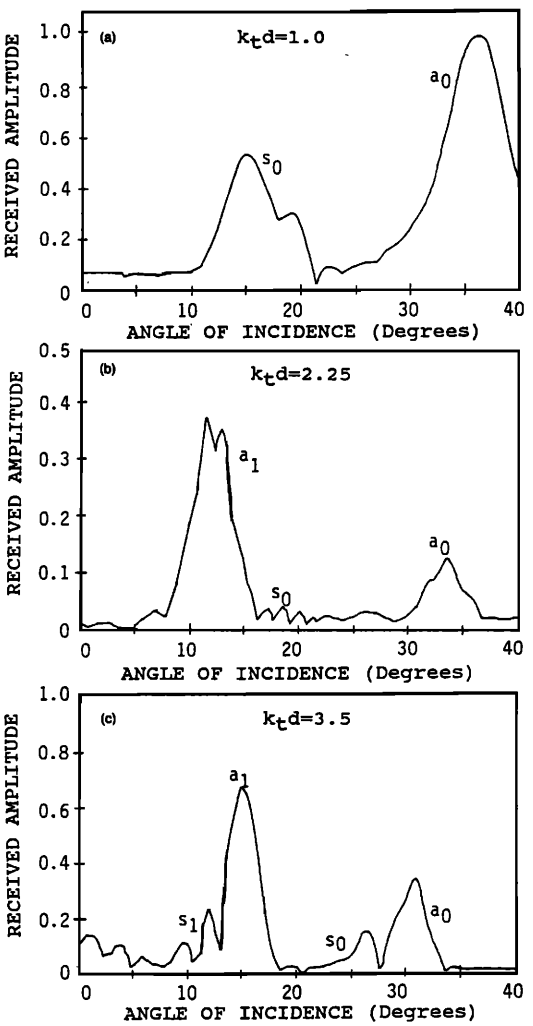

FIG. 6. Received signal amplitude as a function of angle of incidence, at $K_t d = 1.0$, 2.25, and 3.5 for aluminum plate in water.

Two questions arise at this stage regarding these measurements: (1) How do we ensure that the angle at which the measurement is made is the correct Lamb angle? (2) Is the maximum amplitude criterion sufficient to guarantee that the angle is a Lamb angle? These questions are addressed here.

The angle of incidence for the Lamb waves can be checked by a very simple method. Shown in Fig. 7 is the schematic of the signal traveling through the specimen. When the receiver is at its initial location, the total travel time is given by

$$t_i = \frac{l_1}{c_w} + \frac{l_2}{c} + \frac{l_4}{c_w}. \tag{42}$$

As the receiver is moved by a distance x, the travel time becomes

$$t_f = \frac{l_1}{c_w} + \frac{l_2}{c_L} + \frac{l_3}{c_L} + \frac{l_5}{c_w}. \tag{43}$$

The difference in the two arrival times is

$$\Delta t = t_f - t_i = \frac{l_3}{c_L} + \frac{(l_4 - l_5)}{c_w} = \frac{l_3}{c_L} - \frac{x\tan(\theta)}{c_w}$$
$$= x/[c_L \cos(\theta)] - x\tan(\theta)/c_w. \tag{44}$$

When Snell's law, Eq. (40), is substituted in Eq. (44), it is seen that $\Delta t = 0$. This means that at the correct Lamb angle, when the receiver is moved by any arbitrary distance, the total time taken by the wave to travel from the emitter to receiver remains unchanged and only its amplitude is reduced. Hence, in a single experiment, the attenuation is obtained and the correctness of the Lamb angle is verified. The precision of the procedure was found to be 0.1 deg.

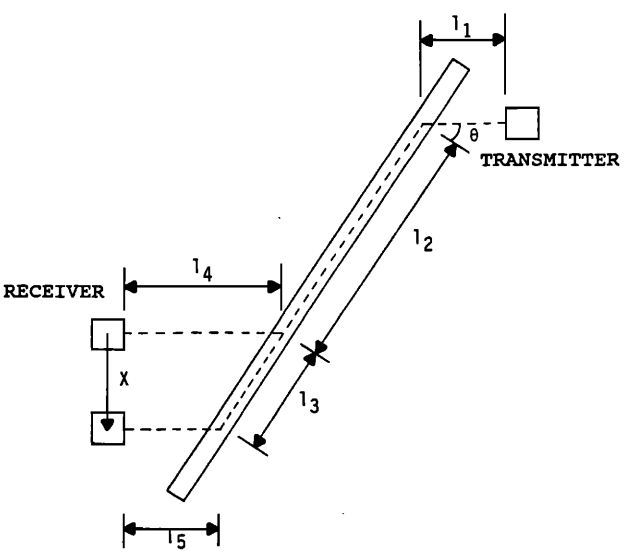

FIG. 7. Travel time for a Lamb wave in a plate.

Next, tests were performed on a $(0/90_3)_s$ graphite/epoxy composite. The dispersion and attenuation curves for this specimen are shown in Fig. 8(a) and (b), respectively. (The derivation of elastic constants for this laminate is deferred to the Appendix.) The experimental results are shown as discrete circles in Fig. 8. The comparison between the theory and experiments is considered reasonable. On the dispersion curves, the comparison does not look very good, but the reason for this discrepancy is as follows. The stiffness coefficients used to solve the dispersion equations are for an ideal composite, with coefficients obtained by the rule of mixtures. Since the laminate used for the tests was fabricated by the author, it is expected that the properties of the laminate will not be as good as the theory suggests. The statically measured stiffness of the laminate is lower and the corresponding wave speed is shown as an arrow in the figure. In view of the reduced value of c_{11} the entire dispersion curves will be shifted downwards and then an excellent agreement between theory and experiment will be observed. This also means that all the elastic constants to be used in the equations should be determined experimentally. Then only, the solution of the dispersion curves will be truly representative of the response of the plate. The low attenuation values shown in Fig. 8(b) could be measured, but then the attenuation rises very rapidly and cannot be measured at higher frequencies due to the reasons described earlier.

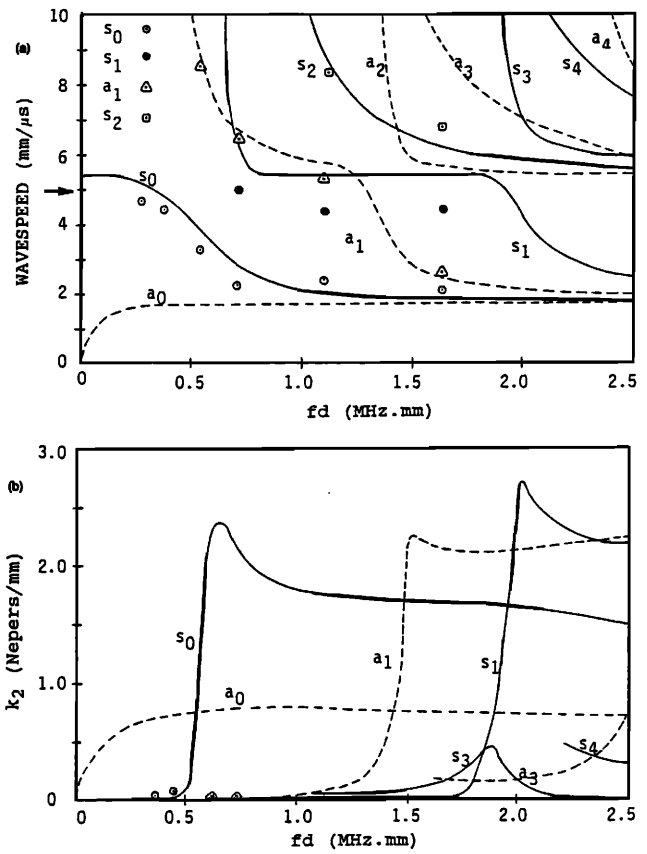

FIG. 8. (a) Dispersion curves and (b) attenuation curves for a $(0/90_3)_s$ laminate in water. Discrete points are experimental.

Finally, in this paper, we have reported theoretical and experimental procedures for investigating leaky Lamb waves in composite laminates. The motivation for this work came from the ultrasonic nondestructive evaluation (UNDE). As a composite laminate is damaged, the stiffness decreases and the attenuation increases. Thus, from a measurement of stiffness and attenuation, one can deduce the extent of damage. Measurement of these quantities in the through-the-thickness direction is a relatively straightforward matter and was the subject of a recent investigation by the present authors (Kinra and Dayal).[25] However, it is of equal, if not greater, interest to measure the in-plane stiffness and attenuation. We have measured these quantities as a function of damage in graphite/epoxy laminates; this will be the subject of a follow-up paper by the authors.

V. CONCLUSIONS

We have considered the propagation of leaky Lamb waves in a balanced symmetric laminate immersed in a liquid. An exact solution for the dispersion equation has been derived. The wave speed and the attenuation were also measured experimentally for a $(0/90_3)_s$ laminate. The agreement between the theory and experiment was found to be quite good.

ACKNOWLEDGMENT

This research was supported by the Air Force of Scientific Research Contract No. F49620-83-C-0067 to Texas A&M University. The program managers were Dr. David Glasgow and Dr. George Haritos.

APPENDIX

The stiffness of an orthotropic lamina is fully defined by the following elastic constants:

$$E_{ijkl} = \begin{pmatrix} E_{1111} & E_{1122} & E_{1133} & 0 & 0 & 0 \\ E_{2211} & E_{2222} & E_{2233} & 0 & 0 & 0 \\ E_{3311} & E_{3322} & E_{3333} & 0 & 0 & 0 \\ 0 & 0 & 0 & E_{2323} & 0 & 0 \\ 0 & 0 & 0 & 0 & E_{3131} & 0 \\ 0 & 0 & 0 & 0 & 0 & E_{1212} \end{pmatrix}. \tag{A1}$$

For a lamina with a fiber orientation in an arbitrary direction, this stiffness tensor has to be written in the rotated coordinate directions. For a fourth-order tensor, the transformation law is

$$T'_{ijkl} = a_{pi} a_{qj} a_{rk} a_{sl} T_{pqrs}, \tag{A2}$$

where a_{ij} is the direction cosine between directions i and j.

Let directions 1 and 2 be in the plane of the plate and a rotation θ takes place about axis 3. Substituting the rotation angle in the transformation law and writing the stiffness in the contracted notation, the following nonzero terms are obtained,

$$E_{jkl} = \begin{pmatrix} C'_{11} & C'_{12} & C'_{13} & 0 & 0 & C'_{16} \\ C'_{21} & C'_{22} & C'_{23} & 0 & 0 & C'_{26} \\ C'_{31} & C'_{32} & C'_{33} & 0 & 0 & C'_{36} \\ 0 & 0 & 0 & C'_{44} & C'_{45} & 0 \\ 0 & 0 & 0 & C'_{54} & C'_{55} & 0 \\ C'_{61} & C'_{62} & C'_{63} & 0 & 0 & C'_{66} \end{pmatrix}. \tag{A3}$$

Only the above terms will be effective when the stiffness matrix is synthesized.[26] Hence, this matrix is used in deriving the governing equations for the Lamb waves. We observe from the main body of derivations of the dispersion equations that the terms left after simplifications are C_{11}, C_{13}, C_{33}, and C_{55}.

Relating the stiffness to modulus properties and the lamina being transversely isotropic, with $E_3 = E_2$ and $\nu_{13} = \nu_{12}$, the following relations are obtained:

$$C_{11} = E_1/(1 - \nu_{12}\nu_{21}),$$
$$C_{13} = \nu_{12}E_2/(1 - \nu_{12}\nu_{21}),$$
$$C_{33} = E_2/(1 - \nu_{12}\nu_{21}),$$
$$C_{55} = G_{13} = G_{12}. \tag{A4}$$

For the AS4/3502 lamina, the following properties were measured:

$$E_1 = 148.0 \text{ GPa},$$
$$E_2 = 11.0 \text{ GPa},$$
$$\nu_{12} = 0.27,$$
$$\nu_{21} = 0.0199,$$
$$G_{12} = 4.83 \text{ GPa},$$

and were used to estimate the laminate properties.

[1]H. Lamb, *On Waves in an Elastic Plate*, Proc. R. Soc. London Ser. A. **93**, 114–128 (1917).

[2]R. D. Mindlin, *Waves and Vibrations in Isotropic Elastic Plates*, Structural Mechanics, edited by J. N. Goodier and N. J. Hoff (Pergamon, New York, 1960).

[3]M. F. M. Osborne and S. D. Hart, "Transmission, Reflection, and Guiding of Exponential Pulse by a Steel Plate in Water. I. Theory," J. Acoust. Soc. Am. **17**, 1–18 (1945).

[4]I. A. Viktorov, *Rayleigh and Lamb Waves* (Plenum, New York, 1987).

[5]J. Krautkramer and H. Krautkramer, *Ultrasonic Testing of Materials* (Springer-Verlag, Berlin), 3rd ed., Chapts. 10–11 (1983).

[6]A. Schoch, "Der Schalldurchgang durch Platten (Sound Transmission in Plates)," Acoustica **2**(1), 1–17 (1952).

[7]L. G. Merkulov, "Damping of Normal Modes in a Plate Immersed in a Liquid," Sov. Phys. Acoust. **10**(2) (1964).

[8]T. J. Plona, M. Bahravesh, and W. G. Mayers, "Rayleigh and Lamb Waves at Liquid Solid Boundaries," Ultrasonics **13**(4), 171–174 (1975).

[9]D. C. Worlton, "Experimental Confirmation of Lamb Waves at Megacycle Frequencies," J. Appl. Phys. **32**(6), 967–971 (1961).

[10]L. R. Dragonnette, "Schlieren Visualization of Radiation Caused by Illumination of Plates with Short Acoustical Pulses," J. Acoust. Soc. Am. **51**(3), 920 (1972).

[11]E. Lehfeldt and P. Höller, "Lamb Waves and Lamination Detection," Ultrasonics **5**, 255–257 (1967).

[12]R. Forito, W. Madigosky, and H. Überall, "Resonance Theory of Acoustic Waves Interacting with an Elastic Plate," J. Acoust. Soc. Am. **66**, 1857–1866 (1979).

[13]M. Hattunen and M. Luukala, "An Investigation of Generalized Lamb Waves Using Ultrasonic Reflectivity Measurements," Appl. Phys. **2**, 257–263 (1973).

[14]R. D. Fay and O. V. Fortier, "Transmission of Sound through Steel Plates Immersed in Water," J. Acoust. Soc. Am. **23**, 339–346 (1951).

[15]A. Freedman, "Reflectivity and Transmissivity of Elastic Plates I. Comparison of Exact and Approximate Theories," J. Sound Vib. **59**(3), 369–393 (1978).

[16]D. S. Choi and A. Bedford, "Transient Pulse Propagation in a Fiber-Reinforced Material," J. Acoust. Soc. Am. **54**, 676–684 (1973).

[17]L. P. Solie and B. A. Auld, "Elastic Waves in Free Anisotropic Plates," J. Acoust. Soc. Am. **54**, 50–65 (1973).

[18]C. C. Habegar, R. W. Mann, and G. A. Baum, "Ultrasonic Plate Waves in Paper," Ultrasonics 57–62 (1979).

[19]R. W. Mann, G. A. Baum, and C. C. Habegar, "Determination of All Nine Orthotropic Elastic Constants for Machine Made Paper," Tech. Assoc. Pulp Paper Ind. **63**(2), 163–166 (1980).

[20]C. T. Sun, J. D. Achenbach, and G. Herrmann, "Continuum Theory of Composite Materials," J. Appl. Mech. 467–475 (1968).

[21]A. Bedford and M. Stern, "Towards a Diffusing Continuum Theory of Composite Materials," J. Appl. Mech. **38**(1), 8–14 (1971).

[22]D. E. Chimenti and A. H. Nayfeh, "Leaky Lamb Waves in Fibrous Composite Laminates," J. Appl. Phys. **58**(12), 4531–4537 (1985).

[23]J. D. Achenbach, *Wave Propagation in Elastic Solids* (North-Holland, Amsterdam, 1973).

[24]J. P. Holman, *Experimental Methods for Engineers* (McGraw-Hill, New York, 1978), Chap. 3, p. 43.

[25]V. K. Kinra and V. Dayal, "A New Technique for Ultrasonic NDE of Thin Specimen," Exp. Mech. **28**(3), 288–297 (1988).

[26]B. D. Agarwal and L. J. Broutman, *Analysis and Performance of Fiber Composites* (Wiley, New York, 1980), Chap. 5, p. 149.